Semi-automated algorithm for segmentation of the trabecular-bone region in micro-MR images of the distal radius and tibia

B. Vasilic[1], F. W. Wehrli[1]

[1]Laboratory for Structural NMR Imaging, Department of Radiology, University of Pennsylvania Medical Center, Philadelphia, PA, United States

INTRODUCTION

Micro-MRI of trabecular bone has significant potential for evaluation of the structural implications of osteoporosis [1] or treatment with antiresorptive or anabolic drugs [2]. Efficient analysis of large clinical studies requires fast and reliable segmentation and registration of the trabecular bone region [3]. Here we have developed a semi-automated segmentation algorithm for micro-MRI images that relies on an operator provided seed point and a cascade of convolution, thresholding, dilation and erosion operations to select the volume of interest. The algorithm was tested for precision, speed and failure rate.

METHODS AND THEORY

Segmentation was performed on in-vivo micro-MRI scans of the distal radius (512×288×32 matrix) and tibia (512×384×32 matrix). The voxel size in both anatomies was $137\times137\times410\mu m^3$. These scans are a part of an ongoing clinical study of bone loss in perimenopausal women. All steps of the algorithm were performed separately on each two-dimensional slice of the acquired volume. In order to select the region of trabecular bone each slice (Fig. 1a) of the scan was first convolved with a 2×2 pixel homogeneous region. The resulting smoothed image (Fig. 1b) was then thresholded (Fig. 1c) with a threshold equal to 99% of the maximum intensity in the smoothed image. To reliably detach the trabecular bone region from the surrounding tissue a series of erosions was applied (Fig. 1d). After eroding the image and using a seed point provided by the operator, the connectivity component belonging to the bone region was selected (Fig. 1e). The manual seed point selection did not slow down the segmentation process since it was done practically instantaneously by the user at the initialization of segmentation. After the bone region was selected, a series of dilation operations (Fig. 1f) were performed to fill in the voids produced in previous thresholding and erosion operations. A Lorentzian smoothing was then applied to smooth out the edges of the mask (Fig. 1g) and the resulting image thresholded (Fig. 1h) to obtain the final shape of the mask. Because of the nature of the initial thresholding step this algorithm has the added advantage of being sensitive to local signal intensities, i.e. local signal to noise ratios (SNR). When shading due to coil inhomogeneities was present, as in the tibia, the algorithm selected regions of the highest SNR in the image. Unfortunately, this also caused the algorithm not to select regions of very high trabecular density (lower signal) albeit at a tolerable rate.

In most scans of the tibia aliasing is present due to the characteristic size of the anatomy relative to the field of view in the phase encoding direction. If surrounding tissue is aliased into the bone region the algorithm incorrectly includes those aliased soft tissue regions into the segmented bone volume. To mitigate this effect we used the fact that segmented regions are mostly continuous along the slice direction. So, the following addition to the main algorithm was performed after the initial segmentation. We will denote the number of slices by z, and index them with k. We will also assume that the aliasing in the middle slice, k_0, does not affect the bone region. The middle slice was then slightly dilated and intersected with the slice above it, k_0+1, and the k_0+1 slice was set to equal this intersection. Assuming continuity, if there was some aliasing in the k_0+1 slice it would not be present in the intersection with the dilated k_0. The same procedure was then applied to the k_0+1 and k_0+2 slice, all the way to the z-1 slice. The same was done in the opposite direction starting from the middle slice, dilating a slice k and intersecting it now with a slice below it, k-1, all the way to the first slice.

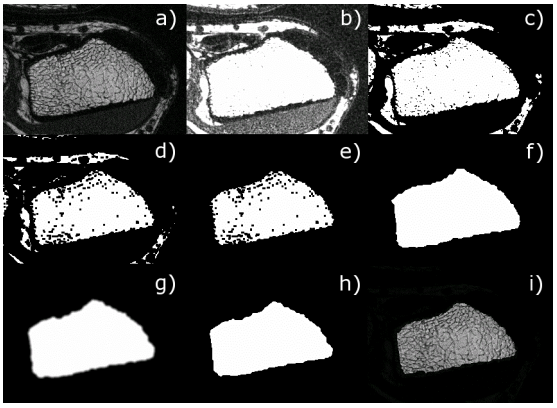

Figure 1. a) Initial image. b) Image blurred with 2x2 kernel. c) Thresholded blurred image. d) Eroded thresholded image. e) Bone connectivity component. f) Dilated connectivity component. g) Dilated connectivity component after blurring. h) Final mask i) Segmented region of the original image.

RESULTS AND CONCLUSION

The algorithm described above was integrated into an existing IDL registration application developed in our laboratory. It was tested for efficiency and reliability on 20 scans of the distal radius and 20 scans of the distal tibia of perimenopausal women. Every segmentation was manually inspected by the operator which took about 30 to 40 seconds. The application was run on a 3.2GHz Pentium 4 under Linux. The average times for wrist and ankle segmentations were 3 and 20 seconds respectively, the ankle segmentations taking more time because of the larger matrix size and the extra time needed to remove regions incorrectly selected due to aliasing. In 16 (80%) of the wrist scans there was no user intervention required after the automatic segmentation. In two of the wrist scans (10%) user intervention was required on two slices where some of the surrounding tissue got incorrectly included in the bone region. In two other wrist scans (10%) low SNR and thick trabeculae caused the algorithm not to select the full bone region so the operator needed to "fill in" the mask manually.

In the ankle, 13 scans (65%) were successfully segmented. All of the 7 (35%) segmentations that required user intervention were caused by periosteal soft tissue incorrectly assigned to bone. However, four of those required adjustment of just one slice at the edge of the selected region where the SNR was low. Two of the 7 failed segmentations required adjustment of two edge slices. Only one failed segmentation, shown in Fig. 2, required manual adjustment of more than one slice since that scan had aliasing in the middle slice and the aliasing correction algorithm failed. The described method reduced the time necessary for segmentation of an individual scan to between 1 and 5 minutes, depending on the anatomical site and the performance of the automation. Since segmentation was one of the most time-intensive operator tasks in the analysis the achieved speedup significantly improved processing efficiency.

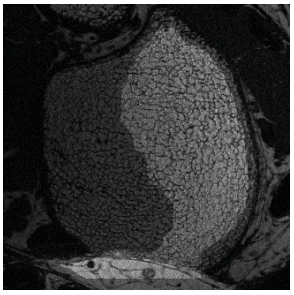

Figure 2. An example of a fat region wrongly assigned to bone due to it being aliased into the trabecular bone region.

[1] M. Kleerekoper et al. Calcif Tissue Int 37: 594, 1985; [2] J. Jiang et al, J Bone Miner Res 18: 1932, 2003; [3] D.C. Newitt et al., Osteo Inter, 2002; 13: 278-87